SELCUK UNIVERSITY JOURNAL OF ENGINEERING SCIENCES

Journal homepage: http://sujes.selcuk.edu.tr

ISSN: 2757-8828

International Open Access

Volume 21
Issue 02

August, 2022

Research Article

Effect of friction coefficients and sliding surface radii on seismic behavior of a triple friction pendulum bearing

Muhamad Zulfakar [a], ***Ali Ihsan Karakas*** [a,*]

[a]*Department of Civil Engineering, Karadeniz Technical University, Trabzon 61080, Turkey*

ARTICLE INFO

Article history:
Received 07 November 2021
Accepted 07 August 2022

Keywords:
Base isolation
Time history analysis
Triple friction pendulum bearing

ABSTRACT

Triple friction pendulum bearing (TFPB) is one of the seismic base isolation devices that are widely used for critical structures prone to severe earthquakes. Some important parameters affecting the seismic performance of a TFPB are effective radius and friction coefficient of sliding surfaces. These parameters need to be investigated parametrically to be able recognize their sensitivities on the efficiency of a bearing. Therefore, in this study, 10 TFPB models with different effective radii and friction coefficients are analyzed numerically. TFPB is modeled as an exact finite element in OpenSees program. The structure supported by the bearings is simply modeled as a mass resting on the TFPB. The bearing models are structurally analyzed using time history analysis method with two ground motion records selected from the PEER Strong Motion Database. The analytical responses of the bearings are obtained for maximum bearing displacements and base shear forces. Also, the hysteretic loops of bearings are acquired to investigate the effects of previously mentioned parameters on the performance of the TFPBs. As far as the numerical results are considered, it can be stated that the bearing displacement and base shear reduce as the radius of the sliding surface increases. On the contrary, when the coefficient of friction is increased, the bearing is subjected to greater base shear. The results also show that the area of the hysteresis loops of the TFPB with smaller effective sliding surface radius is larger. Thus, it can be concluded that the TFPB with larger effective sliding surface radii and smaller friction coefficients performs better for the earthquake motions considered in the present study.

This is an open access article under the CC BY-SA 4.0 license.
(https://creativecommons.org/licenses/by-sa/4.0/)

1. Introduction

Natural disasters are the major causes of structural damages to buildings, as well as economic losses and human deaths. Many new strategies have been developed to enhance the protection of buildings in the face of natural disasters including earthquakes. One of the most effective ways to protect structures in seismically prone areas from earthquake damages is to use seismic base isolation systems. Elastomer ([1], [2], [3]) and friction based bearings ([4], [5], [6], [7]) are basically investigated as isolation systems to reduce seismic responses in structures. The basic idea of the friction based bearings is to create energy dissipation at sliding surfaces by friction damping [8]. In last decades, single, double and triple friction pendulum bearing (TFPB) have been proposed as promising friction based isolation systems [9]. However, many studies have shown that TFPB can provide better seismic isolation performance compared to single and double friction pendulums and elastomer bearings with the same size ([10], [11], [12]). For instance, a building isolated with triple friction pendulum bearings has a better performance than that with single friction pendulum bearings in terms of floor acceleration, inter-story drift, and hysteresis loop responses [13]. Also, Morgan and Mahin [14] suggested that TFPBs are ideal for performance-based design of structures and they have the ability to provide large displacements with smaller devices compared to single or double pendulum bearings. Therefore, this study focuses on seismic behavior of a triple friction pendulum bearing.

* Corresponding author. E-mail address: aliihsan.karakas@ktu.edu.tr

The geometric characteristics of a typical TFPB are shown in Figure 1 [10]. It can be seen that a relatively small inner slider can move between two articulated sliders which can move between top and bottom plates. The sliding surfaces of sliders and plates are spherical. The frictions between these surfaces prevent motion due to small horizontal loads and consume energy by sliding between surfaces due to large horizontal loads. A restoring force is generated with the help of vertical load on the bearing and curvatures of the sliding concave surfaces when horizontal displacement occurs. Appropriate friction coefficients and friction surface radii must be selected to be able to have various pendulum mechanisms for different earthquake levels [10].

The effective radii and coefficients of friction of the sliding surfaces are important parameters that determine the performance of a TFPB. The selection of an optimal set of TFPB design variables, such as sliding surface radii, friction coefficients, and displacement capacity of each concave surface is an important step because their optimal performances are dependent on the ground motion properties and the superstructure's seismic performance objectives [15]. In this study, several TFPB models with different effective radii and friction coefficients are analyzed considering two different ground motions in time history analysis to investigate the effects of these parameters on the dynamic behavior of a TFPB.

2. Research Methodologies

For triple friction pendulum bearing, the geometric characteristics that dictate behavior of seismic isolation performance are shown in Figure 1. Surface radius of curvatures (R_i), coefficients of frictions (μ_i), the displacement capacity of each surface (d_i) and finally the distance between the center point of the slider and the spherical surface and the pivot point of the articulated slider (h_i) by which the effective curvature is calculated ($R_{eff\,i} = R_i - h_i$) are shown in the figure.

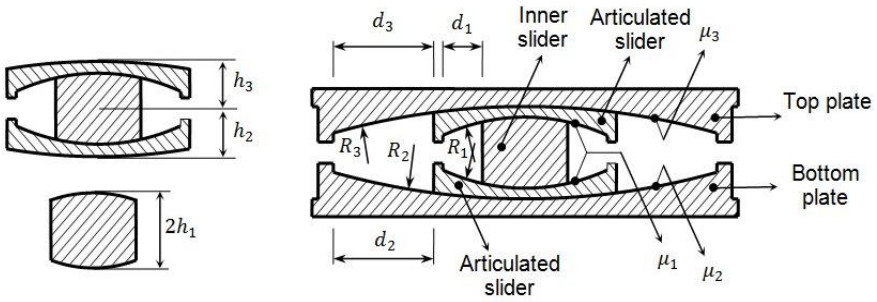


Figure 1. Cross section of a TFPB

The unidirectional backbone curve for horizontal force-deformation of a generalized triple pendulum bearing can be divided into 5 stages as shown in Figure 2 [10]. Note that in Figure 2, the normalized horizontal force $f = F/W$ is used and the curve is called normalized backbone curve [16]. The bearing dimensions and friction coefficients must satisfy the following conditions [10]:

$$R_{eff1} < R_{eff2} < R_{eff3} \quad (1)$$

$$\mu_1 < \mu_2 < \mu_3 \quad (2)$$

$$d_1 > (\mu_3 - \mu_1)R_{eff1} \quad (3)$$

$$\mu_3 < \frac{d_1}{R_{eff1}} + \mu_1 \quad (4)$$

The constraint on the pendulum lengths (Equation (1)) must be satisfied so that the bearing is activated with high stiffness at small earthquakes and lower stiffness at moderate earthquakes. Constraint on the friction coefficients (Equation (2)) guarantees the sequence of sliding, engaging in this order: inner slider, lower articulated slider, and upper articulated slider. Constraint of Equation (3) guarantees that the displacement limits are reached on articulated sliders before the inner slider to activate the stiffening stage at the end of the backbone curve. The constraint of Equation (4) guarantees that sliding occurs on all surfaces before the bearing goes into a stiffening stage.

Five stages of sliding are shown in Figure 3 [10]. Explanations of these stages are given as [17]:

Stage 1: When the horizontal force exceeds the frictional force between the inner slider and the lower articulated slider, which is equal to the frictional force between the inner slider and the upper articulated slider, the inner slider will slide between the two sliders.

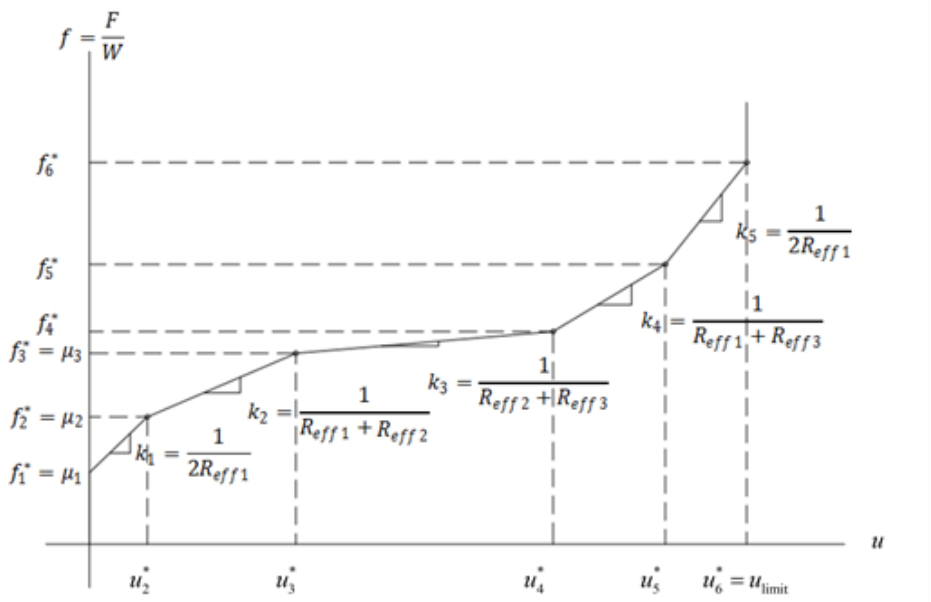


Figure 2. Normalized backbone curve for TFPB

Stage 2: When the normalized horizontal force exceeds μ_2, relative sliding will occur between the articulated slider and bottom concave plate. Sliding on the contact surface between the inner slider and the upper articulated slider also does not set sliding between the upper slider and the convex plate. The inner slider must slide to increase the slope to balance the increase in horizontal force. The inner slider stops sliding on the lower articulated slider because the increasing horizontal force is balanced by the inclination of the inner slider and the lower articulated slider on the lower concave plate rather than by the sliding of the inner slider on the articulated slider. In other words, the increasing horizontal force in this stage is provided by the increased inclination of the inner slider. At the upper part of the inner slider, this inclination is provided by the sliding between the inner slider and the upper articulated slider. At the lower part of the inner slider, the inclination is created by the sliding between the lower articulated slider and the lower concave plate.

Stage 3: When the horizontal force exceeds the frictional force between the upper articulated slider and the upper concave plate, sliding occurs between the components. At this stage, the lower articulated slider continues to slide on the lower concave plate, but sliding between the inner slider and the upper articulated slider stops. The increasing horizontal force is caused by the increasing inclination of the inner slider due to the sliding of the two articulated sliders on the two concave plates above and below.

Stage 4: At this stage the lower articulated slider reaches its displacement limit and cannot continue to slide on the lower concave plate. This forces the inner slider to slide on the lower articulated slider, increasing the inclination of the inner slider so that the bearing can accommodate the increasing horizontal force. The upper articulated slider has not yet reached the limit and there is no relative sliding between the inner slider and the upper articulated slider.

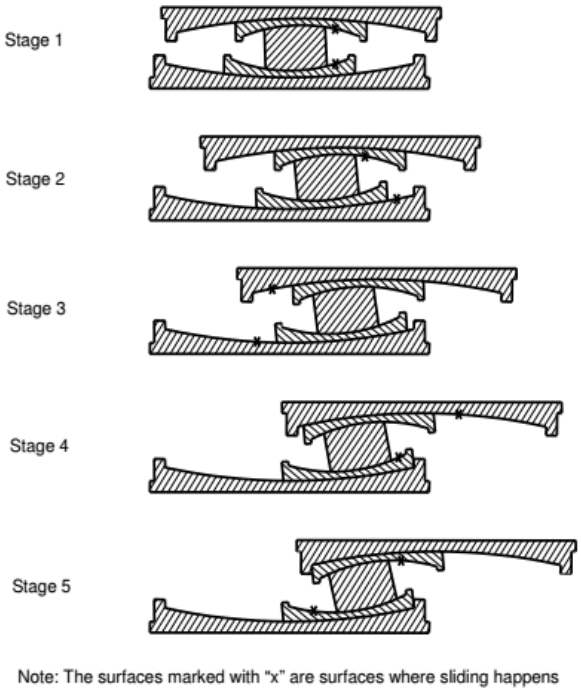


Figure 3. Five stages of TFPB sliding

Stage 5: At this stage, the upper articulated slider reaches its displacement limit and cannot go further on the upper concave plate. As a result, the inner slider is forced to slide on the upper articulated slider to provide the increasing inclination to support the increasing horizontal force. When the inner slider contacts the displacement restraining rings of the articulated sliders, the bearing reaches its displacement limit and cannot go further.

Figure 4 shows a simplified representation of series single friction pendulum (SFP) elements used to model the five-stage behavior of a TFPB [10]. Each element in the series model is composed of a parallel arrangement of a linear spring with stiffness equal to $1/R_{effi}$, a velocity-dependent perfectly plastic friction element represented by the modified Bouc-Wen model with the coefficient of friction equal to μ_i, and a gap element with displacement capacity of d_i. Therefore, the force produced by the i[th] isolator element in the x direction is given by [18]:

$$F_i = \frac{W_i}{R_{effi}} u_i + \mu_i W_i Z_i + k_{ri}(|u_i| - d_i) sign(u_i) H(|u_i| - d_i) \quad (5)$$

where W_i is the mass supported by each isolator, u_i is the relative displacement of SFP element in the x direction, k_{ri} is the stiffness after gap closing, which should be assigned a large value, H denotes the Heaviside function and Z_i denotes a dimensionless variable of i[th] element along the x direction.

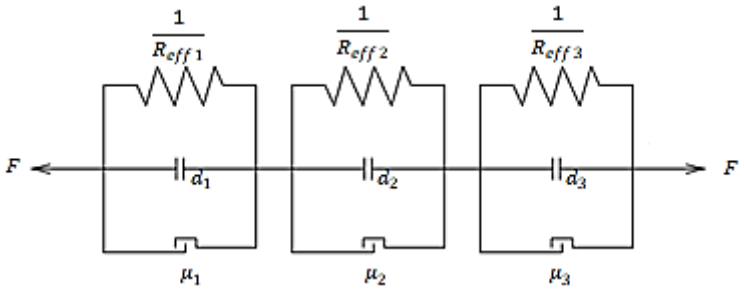


Figure 4. Spring friction pendulum elements in series to model a TFPB

The spring element stands for the restoring force due the curvature of the spherical surfaces. A gap element is used to restrict displacement capacity of each sliding surface This serially connected spring element is now available for general use in OpenSees program to model TFPB isolators [19]. This series spring element is used in this study to obtain the behaviors of different TFPB models described below.

There are 10 models that have been analyzed in order to investigate the effects of friction coefficients and sliding surface radii on the behavior of TFPB with a superstructure weight of W=100 kN. There are two different friction coefficient compositions (μ_1: μ_2: μ_3) used in this analysis, the first and second compositions are denoted by U1 and U2 in the names of the models, respectively. The first composition (U1) of the friction coefficients is 0.02: 0.04: 0.06, and the second composition (U2) is 0.02: 0.06: 0.12. The radii of the top and bottom plates are assumed to be the same and larger than the radius of the articulated slider which is 400 mm. The radii of the top and bottom plates are altered as given in Table 1 and the radius value is given in the names of the models in meter. The details of the models can be seen in Table 1.

Table 1. Model Parameters

Model	R_{eff1} (mm)	R_{eff2} (mm)	R_{eff3} (mm)	μ_1	μ_2	μ_3	d_1 (mm)	d_2 (mm)	d_3 (mm)
R1.34_U1		1340	1340						
R1.84_U1		1840	1840						
R2.34_U1	400	2340	2340	0.02	0.04	0.06	40	265	265
R2.84_U1		2840	2840						
R3.34_U1		3340	3340						
R1.34_U2		1340	1340						
R1.84_U2		1840	1840						
R2.34_U2	400	2340	2340	0.02	0.06	0.12	40	265	265
R2.84_U2		2840	2840						
R3.34_U2		3340	3340						

The two ground motions which are Imperial Valley-02, 5/19/1940 at El Centro Array #9 station with a magnitude of 6.95 and Kobe Japan, 1/16/1995, at Abeno station with a magnitude of 6.90 were selected from the PEER Strong Motion Database [20]. The time-acceleration records of the earthquakes are shown in Figure 5. It can be seen from

the graphs that the Kobe and Imparial Valley earthquakes have near-fault and far-fault ground motion characteristics, respectively, even they have close peak ground accelerations. Thus, the effects of ground motions with different frequency profile on the dynamic behavior of the bearing can also be investigated.

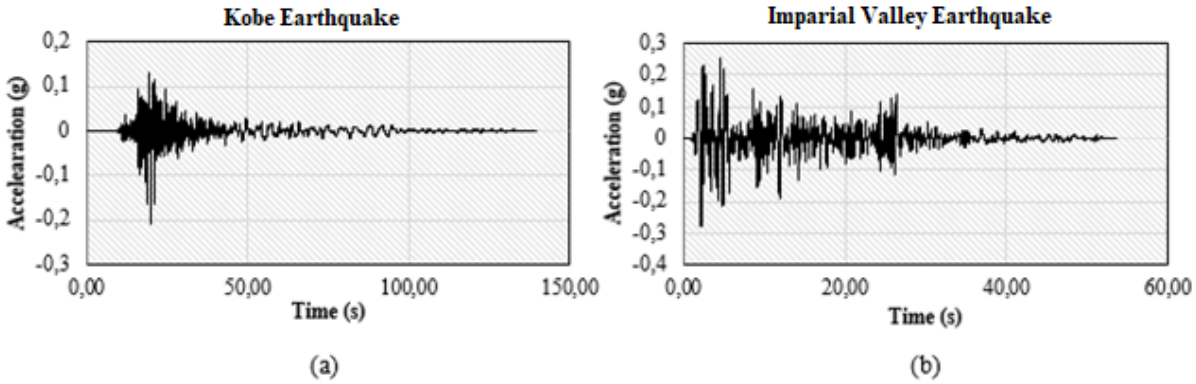


Figure 5. Acceleration records for (a) Kobe and (b) Imperial Valley earthquakes

3. Results and Discussions

The maximum displacements and base shear forces obtained from the TFPB analyses performed for Kobe earthquake are shown in Figure 6. It can be seen from the results that when the friction coefficients of the top and bottom plates are increased it causes larger displacements. The percentage increase in maximum displacements under Kobe earthquake excitation as the friction coefficient is changed from U1(0.02: 0.04: 0.06) to U2(0.02: 0.06: 0.12) are 0.44%, 1.67%, 2.39%, 3.91% and 4.83% for effective sliding surface radius R1.34, R1.84, R2.34, R2.84 and R3.34, respectively. Thus, it can be stated that a change in friction coefficients has a vital effect when the sliding surface radius is larger. Figure 6 also shows that increasing the effective surface radius results in smaller maximum displacement and maximum base shear for the first composition of friction coefficients (U1) under the Kobe earthquake excitation. However, while an increase in the effective sliding surface radius reduces the maximum base shear it increases the maximum displacement for the second composition of friction coefficients (U2).

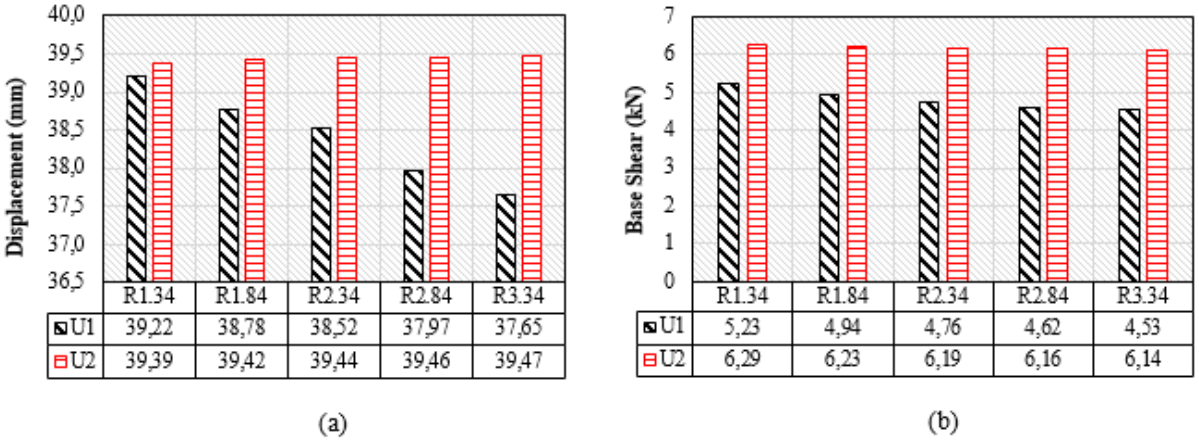


Figure 6. Seismic responses as maximum (a) displacement and (b) base shear for Kobe earthquake

Figure 7 depicts the maximum displacements and base shear forces for the analyses of TFPB subjected to Imperial Valley -02 earthquake. In Figure 7(a), when the coefficient of friction is increased from U1 to U2 for effective radius R1.34, the displacement decreases by 6.66% from 122.55 mm to 114.40 mm. Similarly, for effective radius R1.84, the displacement decreases by 3.17% from 120.53 mm to 116.71 mm. However, for the next three effective radii, larger displacements are obtained by increasing the coefficient of friction. The maximum displacement differences for Imperial Valley earthquake excitation in the case that the friction coefficient is altered from U1 to U2 are -6.66%, -3.17%, 1.49%, 5.07% and 8.16% for each effective sliding surface radius, respectively. So, it can not be directly said that an increase in friction coeffcients does not result in an increase in displacement but it depends on the earthquake ground motion profile which activates different stages of bearings for different sliding surface radius. Figure 7 also shows that while an increase in the effective surface radius leads to a smaller maximum

displacement and base shear for the composition U1, it increases the maximum displacement but reduces the maximum base shear for the composition U2.

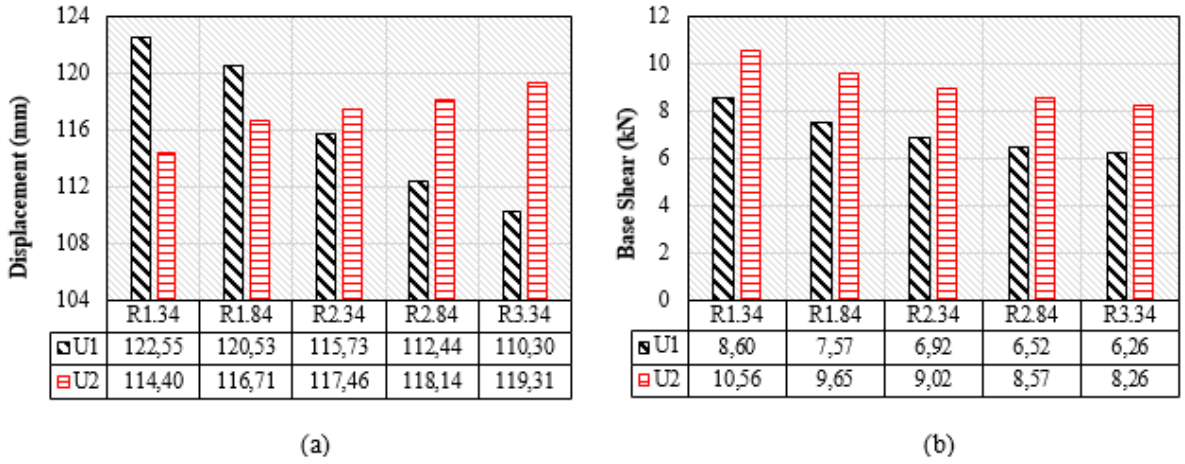


Figure 7. Seismic responses as maximum (a) displacement and (b) base shear for Imperial Valley earthquake

Figure 8 displays hysteresis loops of the friction pendulum bearing under Kobe earthquake. Hysteretic loops illustrate the force-displacement responses of friction pendulum bearings. Area of hysteresis loop can be used to determine the energy dissipation per cycle and the effective damping provided by the bearing. Figure 8 indicates that the TFPB with the smallest effective sliding surface radius has a greater peak isolator displacement than the others, as well as a larger base shear. Figure 8 also shows that the TFPB with the smallest effective sliding surface radius has a slightly larger hysteresis loop (dissipation energy) than the other TFPBs.

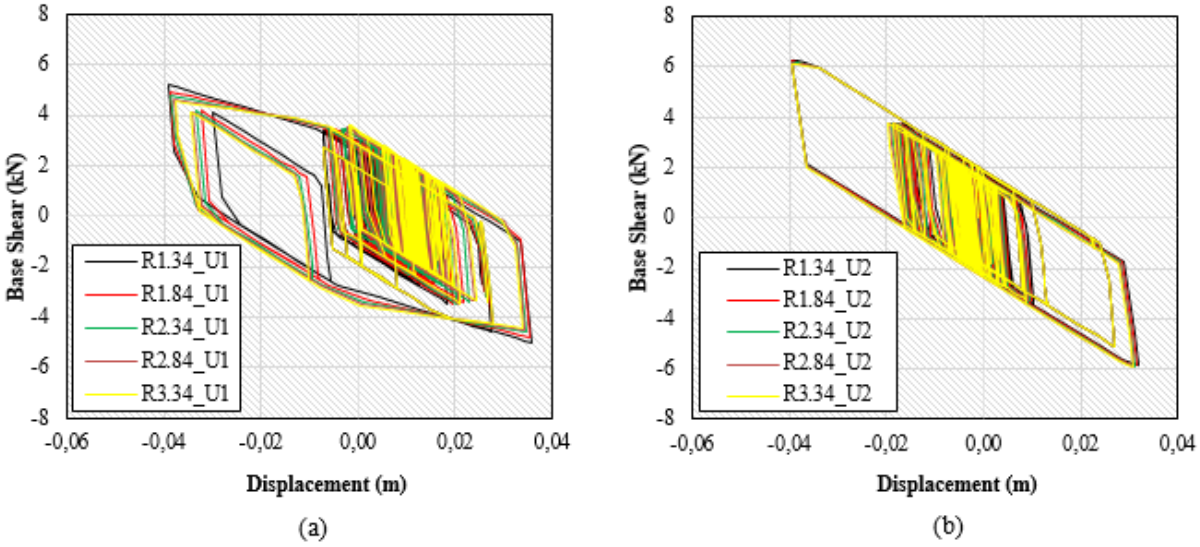


Figure 8. Hysteresis loops for the (a) first (U1) and (b) second (U2) compositions of friction coefficients due to Kobe earthquake

Similarly, Figure 9 shows the hysteresis loops of the pendulum bearings under Imperial Valley -02 earthquake. When compared with the hysteresis loops for the Kobe earthquake, it can be realized that the effects of the surface radius on the loops are noticeable due to the larger accelerations of Imperial Valley earthquake records. Also, it can be easily realized that the TFPB with the smallest effective sliding surface radius has a larger peak isolator displacement than the others, as well as a greater base shear for the first composition of friction coefficient (U1). However, Figure 9(b) depicts that the TFPB with the largest effective sliding surface radius has the largest peak isolator displacement than the others but the smallest base shear for the second composition of friction coefficient (U2). Additionally, it can be stated that the amount of dissipated energy is greater when the maksimum ground displacement of the earthquake is larger since such strong earthquakes activate different stages of the sliding regime of TFPB which generate additional energy consumption in the system.

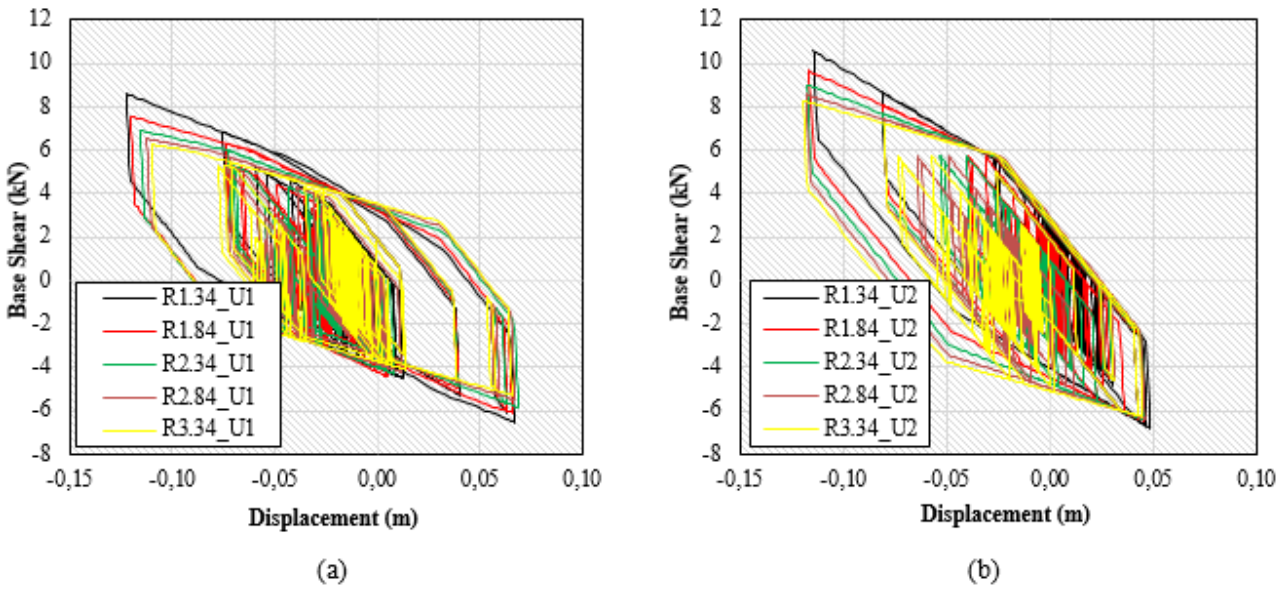


Figure 9. Hysteresis loops for the (a) first (U1) and (b) second (U2) composition of friction coefficients due to Imperial Valley earthquake

4. Conclusions

In this study, triple friction pendulum bearing (TFPB) models with different friction coefficient compositions (μ1: μ2: μ3) denoted by U1 (0.02: 0.04: 0.06) and U2 (0.02: 0.06: 0.12) and sliding top and bottom plate surface effective radii altering between 134 mm and 334 mm have been investigated analitically using time history analysis for two different earthquakes which are Kobe and Imparial Valley earthquakes. The TFPB has been modeled as a special series of single friction pendulum spring finite elements in OpenSees program.

The numerical analysis results indicate that while an increase in the effective surface radius generates smaller maximum base shear and displacement for the first composition (U1) of friction coefficient it reduces the maximum base shear but increases the maximum displacement for the second composition (U2). Additionaly, when the coefficient of friction is increased from U1 to U2 the trend of change in the maximum displacement depends on the effective surface radius as well as earthquake ground motion considered. That is, the maximum displacement increases for all surface radii under Kobe earthquake but decreases for smaller radii under Imperial Valley earthquake. The results also show that the area of hysteresis loops (dissipation energy) of the TFPB with smaller effective sliding surface radius is larger than those of other TFPBs. As a final remark it can be stated that the TFPB with larger effective sliding surface radius and smaller friction coefficients performs better for different earthquake levels considered in the study.

Acknowledgment

The authors received no financial support for the research, authorship and/or publication of this article.

Author contributions

Conceptualization: [Ali Ihsan Karakas]; Methodology: [Muhamad Zulfakar]; Formal analysis and investigation: [Muhamad Zulfakar]; Writing - original draft preparation: [Muhamad Zulfakar]; Writing - review and editing: [Ali Ihsan Karakas]; Resources: [Muhamad Zulfakar]; Supervision: [Ali Ihsan Karakas]

Conflicts of interest/Competing interests

There is no conflict of interest or common interest with any institution or person that we know that could affect our work.

References

[1] F. Naiem and J. Kelly, Design of Seismic Isolated Structures From Thery To Practice, New York: John Willey and Sons, 1999.

[2] E. Tubaldi, S. Mitoulis and H. Ahmadi, "Comparison of Different Models for High Damping Rubber Bearing in Seismically Isolated Bridges," *Soil Dynamics and Earthquake Engineering*, pp. 329-345, 2018.

[3] E. Neethu, "Effect of Dynamic Soil-Structure Interaction on the Seismic Response of Bridges with Elastomeric Bearings," *Asian Journal of Civil Engineering*, pp. 197-207, 2019.

[4] M. K. Shrimali and R. S. Jangid, "Seismic response of liquid storage tanks isolated by sliding bearings," *Engineering Structures*, vol. 24, no. 7, p. 909–921, 2002.

[5] V. Zayas, S. Low and S. Mahin, "A simple pendulum technique for achieving seismic isolation," *Earthquake Spectra*, vol. 6, no. 2, p. 317–333, 1990.

[6] N. V. Nguyen, H. P. Hoang and K. t. Huong, "Performance of Single Friction Pendulum Bearing for Isolated Buildings

Subjected to Seismic Actions in Vietnam," in *IOP Conference Series: Earth and Environmental Science*, 2018.

[7] J. C. Reyes, M. T. Herrera, J. Paul Smith-Pardo and L. S. Cordoba, "Effective Live Load Mass for Storage Buildings on Friction Pendulum Isolators," *Engineering Structures*, vol. 218, no. May, p. 110843, 2020.

[8] T. C. Becker and S. A. Mahin, "Experimental and analytical study of the bi-directional behavior of the triple friction pendulum isolator," *Earthquake Engineering and Structural Dynamics*, vol. 41, no. 3, pp. 355-375, 2012.

[9] D. M. Fenz and M. C. Constantinou, "Modeling triple friction pendulum bearings for response-history analysis.," *Earthquake Spectra*, vol. 24, no. 4, p. 1011–1028, 2008a.

[10] N. D. Dao, *Seismic Response of a Full-scale 5-story Steel Frame Building Isolated by Triple Pendulum Bearings under 3D Excitations*, PhD Theses: University of Nevada, 2012.

[11] M. Yurdakul and Ş. Ateş, "Modeling of Triple Concave Friction Pendulum Bearings for Seismic Isolation of Buildings," *Structural Engineering and Mechanics*, vol. 40, no. 3, pp. 315-334, 2011.

[12] M. Malekzadeh and T. Taghikhany, "Multi-stage Performance of Seismically Isolated Bridge Using Triple Pendulum Bearings," *Advances in Structural Engineering*, vol. 15, no. 7, pp. 1181-1196, 2012.

[13] Y. Xu, T. Guo and P. Yan, "Design optimization of triple friction pendulums for base-isolated high-rise buildings," *Advances in Structural Engineering*, vol. 22, no. 13, p. 2727–2740, 2019.

[14] T. A. Morgan and S. A. Mahin, "The Use of Base Isolation Systems to Achieve Complex Seismic Performance Objectives," Tokyo Institute of Technology, 2011.

[15] Y. Xu, T. Guo, P. Yan and A. Li, "Effect of Semiactive Control on Wind and Seismic Responses of High-Rise Building Supported on Triple Friction Pendulums," *Journal of Performance of Constructed Facilities*, vol. 34, no. 3, p. 04020035, 2020.

[16] D. M. Fenz and M. C. Constantinou, "Spherical sliding isolation bearings with adaptive behavior: Theory," *Earthquake Engineering and Structural Dynamics*, vol. 37, no. 2, p. 163–183, 2008b.

[17] H. Moeindarbari and T. Taghikhany, "Seismic optimum design of triple friction pendulum bearing subjected to near-fault pulse-like ground motions," *Structural and Multidisciplinary Optimization*, vol. 50, no. 4, p. 701–716, 2014.

[18] P. Namiranian, G. Ghodrati Amiri and S. Veismoradi, "Near-fault seismic performance of triple variable friction pendulum bearing," *Journal of Vibroengineering*, vol. 18, no. 4, p. 2293–2303, 2016.

[19] F. McKenna, G. L. Fenves and M. H. Scott, "Open System for Earthquake Engineering Simulation," University of California, Berkeley, 2000.

[20] PEER, "Pacific Earthquake Enginnering Research Center," University of California, Berkeley, 2021.